

Validation of Sea Ice Motion from QuikSCAT with those from SSM/I and Buoy

Yunhe Zhao, Antony K. Liu, and David G. Long, *Senior Member, IEEE*

Abstract—Arctic sea ice motion for the period from October 1999 to March 2000 derived from QuikSCAT and special sensor microwave/imager (SSM/I) data using the wavelet analysis method agrees well with ocean buoy observations. Results from QuikSCAT and SSM/I are compatible when compared with buoy observations and complement each other. Sea ice drift merged from daily results from QuikSCAT, SSM/I, and buoy data gives more complete coverage of sea ice motion. Based on observations of six months of sea ice motion maps, the sea ice motion maps in the Arctic derived from QuikSCAT data appear to have smoother (less noisy) patterns than those from NSCAT, especially in boundary areas, possibly due to constant radar scanning incidence angle. For late summer, QuikSCAT data can provide good sea ice motion information in the Arctic as early as the beginning of September. For early summer, QuikSCAT can provide at least partial sea ice motion information until mid-June. In the Antarctic, a case study shows that sea ice motion derived from QuikSCAT data is consistent with pressure field contours.

Index Terms—QuikSCAT, sea ice motion, special sensor microwave/imager (SSM/I), wavelet transform.

I. INTRODUCTION

QUICKSCAT, a “quick recovery” mission to fill the gap created by the loss of data from the NASA Scatterometer (NSCAT), when the ADEOS-1 satellite lost power in June 1997, was launched on June 19, 1999. QuikSCAT is an active sensor, and the sensor footprint is an ellipse $25 \text{ km} \times 37 \text{ km}$. In both the Arctic and the Antarctic regions, repeated footprints of the satellite make it possible to construct QuikSCAT images with a 12.5 km grid and finer resolution (e.g., see [1]). In this paper, the daily (estimated over a four-day sliding window for the Arctic and over a one-day sliding window for the Antarctic) sea ice motion derived from QuikSCAT using an ice-tracking algorithm based on wavelet transform is demonstrated, and the applications of the daily sea ice motion are indicated. The uncertainty of QuikSCAT-derived sea ice motion is determined from validation with those from *in situ* buoy data and Defense Meteorological Satellite Program (DMSP) special sensor microwave/imager (SSM/I) observations during the same period of time. The instrument differences between QuikSCAT and NSCAT lead to significantly different spatial and temporal sampling characteristics, and it is for this reason that QuikSCAT ice motion validation is required. NSCAT is a fan-beam scatterometer with fixed azimuth but variable incidence, while QuikSCAT has fixed incidence and variable azimuth.

Satellite observations provide more complete and routine coverage of polar region than observations from any other means, and they have been used by several authors in deriving polar sea ice drift (e.g., see [2] and references cited there). The efficiency and utility of wavelet transform in analyzing

nonlinear dynamical ocean systems has also been documented in several papers ([2] and references cited there). In Section II, wavelet analysis for ice feature tracking and sea ice motion from QuikSCAT and SSM/I data are presented. Wavelet analysis results from QuikSCAT and SSM/I are compared with the ice motion derived from buoys for validation in Section III. Section IV deals with the potential application of QuikSCAT data in summer ice tracking. Section V is devoted to a sea-ice-tracking case study for the Antarctic using QuikSCAT data. The results and applications of satellite-derived sea ice motion are discussed and summarized with previous NSCAT and SSM/I data in the final section.

II. WAVELET ANALYSIS OF SATELLITE IMAGES

A sea-ice-tracking procedure based on wavelet transform of satellite data and its error analysis have appeared in [2]–[4]. The effect of wavelet transform is a bandpass filter with a threshold for feature detection. For the details of the procedure, we refer readers to [2]–[4]. In this study, the same procedure is applied to QuikSCAT and SSM/I data with a few modifications. For the Arctic, QuikSCAT images with 12.5 km pixel size are first constructed from QuikSCAT Level 2A data, and SSM/I images are obtained from SSM/I compact discs. QuikSCAT Sigma-0 data has an incidence angle either around 54.24° (*v*-polarization) or around 46.44° (*h*-polarization) within $\pm 0.5^\circ$. Only *v*-polarization Sigma-0 data with an incidence angle around 54.24° are used in the construction of QuikSCAT images because of its better coverage. Areas indicated by sea ice flags in QuikSCAT data as land, open ocean, or no-data areas are masked in the images. For the Antarctic case study, the QuikSCAT data are processed with a scatterometer image reconstruction (SIR) resolution enhancement algorithm to a pixel resolution of 4.45 km from QuikSCAT Level 1B data [1], and sea ice extent is determined using the method of [5]. The QuikSCAT design specifications for location accuracy requirements are 25 km (rms) absolute and 10 km (rms) relative. However, the actual performance is currently estimated to be better than 6 km (rms) absolute and less than 1 km (rms) relative with bias dominating the total error [6]. Thus, QuikSCAT has very high precision measurement locations, far exceeding its design specifications and enabling the application of resolution enhancement algorithms. For both cases, wavelet transform is then applied to the satellite image at various scales to separate various ice textures or features. In the Arctic, two tracking regions are considered: coast/bay for fast ice motion (with a two-day sliding window), and central Arctic for slow ice motion (with a four-day sliding window). Template matching is performed with the results from the wavelet transform of the images between day 1 and day 5 for the central Arctic and between day 2 and day 4 for the coast/bay.

In the Antarctic, template matching is performed with the results from the wavelet transform of the images between day 1 and day 2. For both cases, velocities are estimated by dividing the displacement over the time interval. Finally, the sea ice drift map can be merged by block average with outlier filtering. The outlier filtering after block average is performed as follows: at any location, the mean velocity of nine neighboring ice velocities is computed. If the angle between the mean ice velocity and the ice velocity at the location is bigger than a certain degree, then the ice velocity at the location is discarded.

Fig. 1(a) and (b) show sea ice drift maps of the Arctic Ocean for November 5, 1999, derived from SSM/I and QuikSCAT data, respectively, where thin white arrows indicate velocities derived from satellite data, while thick white arrows indicate velocities derived from buoy data. Two circulation patterns—one in the Beaufort Sea and the other across the Chukchi, Beaufort, and Laptev Seas—are clearly observed in the maps. The ice motion converges in an area between the Chukchi Sea and the Beaufort Sea. Notice that velocities derived from both QuikSCAT and SSM/I data agree well with those from buoy data. Wavelet transform scales used in deriving these images from QuikSCAT and SSM/I data are based on parameter study and testing and are 1.0, 2.42, and 2.828. The resultant ice velocities have been block averaged to a $100 \text{ km} \times 100 \text{ km}$ grid with outlier filtering. The empty areas with no velocity in the map indicate the regions where the tracking procedure cannot be used, since no matching templates between the time periods can be determined. Clearly, the ice motion maps derived from QuikSCAT and SSM/I data for November 5, 1999 are complementary to each other. The regions without ice velocity data from QuikSCAT and SSM/I are generally not colocated, since the QuikSCAT and SSM/I data correspond to different physical features: surface roughness and brightness-temperature anomalies, respectively. For the period from October 1999 to March 2000, based on the observations of sea ice motion maps, the patterns of motion from QuikSCAT appear smoother than those from SSM/I.

VI. DISCUSSION

To further examine satellite-data-derived sea ice motion, Table I summarizes some six-month comparison results of sea ice motion derived from SSM/I, NSCAT, and QuikSCAT with those derived from buoy data for different periods. For all comparison periods, the rms of the speed differences between buoy-derived ice velocities and satellite-derived ones are all under 3 cm/s, and the rms of the direction differences between them are around 30° . Moreover, all satellite-derived sea ice motion data sets are consistent and comparable.

It is clear that sea ice motion products derived from SSM/I, NSCAT, and QuikSCAT data have very good quantitative agreements with the ice motion products derived from buoy data. But, the sea ice motion products derived from NSCAT and QuikSCAT data are slightly more accurate than that derived from SSM/I data because both NSCAT and QuikSCAT are active sensors and do not suffer from cloud and atmospheric effects. Also, the results from NSCAT and QuikSCAT are very consistent. The rms of the direction difference between NSCAT-derived and buoy-derived ice drift for the period from October, 1996 to March, 1997 is slightly better than that

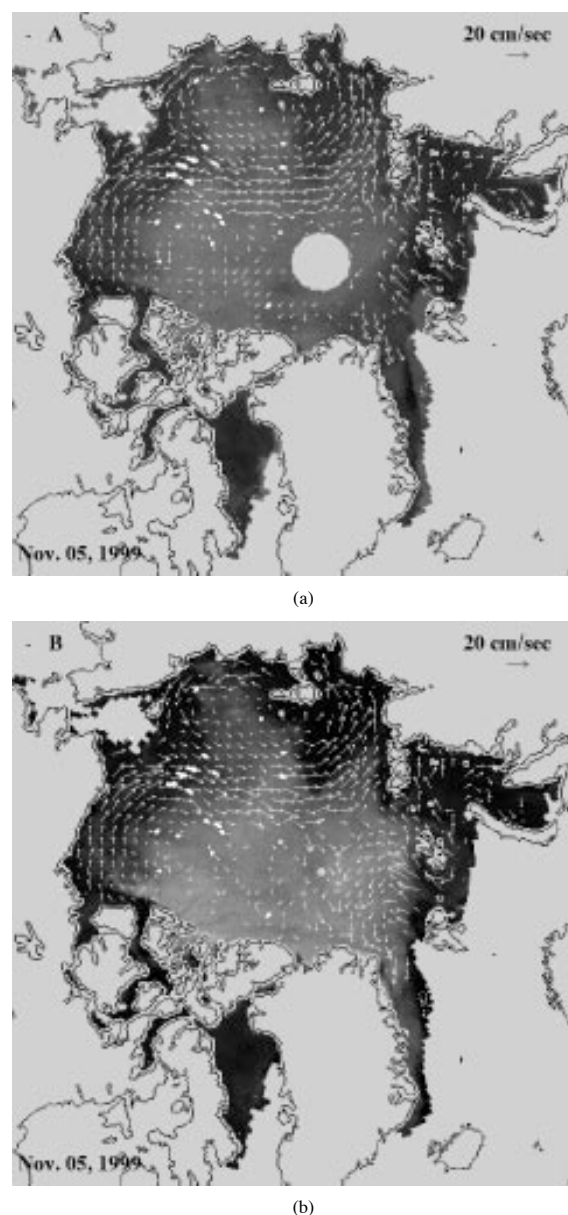


Fig. 1. Arctic sea ice drift maps of the Arctic basin in a grid of $100 \times 100 \text{ km}$ derived from (a) SSM/I 85 GHz radiance data and (b) from QuikSCAT data on November 5, 1999. Thin white arrows indicate velocities derived from feature tracking using wavelet analysis, while thick white arrows indicate velocities from buoys.

between QuikSCAT-derived ice velocities and buoy-derived ones for the same winter period in 1999 and 2000. But keep in mind that the rms are for two different periods and that the ice motion in the central Arctic during winter 1999 has a very slow motion, and so the ice-tracking results are less accurate. In fact, based on the observations, the ice motion maps from QuikSCAT data appear to have smoother patterns than those from NSCAT, especially in boundary areas, e.g., in the Kara and Barents Seas where there is no buoy for comparison.